

Seer: Proactive Revenue-Aware Scheduling for Live Streaming Services in Crowdsourced Cloud-Edge Platforms

Shaoyuan Huang[†], Zheng Wang[†], Zhongtian Zhang[†], Heng Zhang[†], Xiaofei Wang^{†*}, Wenyu Wang[§]

[†]College of Intelligence and Computing, Tianjin University, Tianjin, China

[§]PPIO Cloud Computing (Shanghai) Co., Ltd., Shanghai, China

{hsy_23, wz_424, 3021210045, hengzhang, xiaofeiwang}@tju.edu.cn, wayne@pplabs.org

arXiv:2402.14619v1 [cs.DC] 22 Feb 2024

Abstract—As live streaming services skyrocket, Crowdsourced Cloud-edge service Platforms (CCPs) have surfaced as pivotal intermediaries catering to the mounting demand. Despite the role of stream scheduling to CCPs’ Quality of Service (QoS) and throughput, conventional optimization strategies struggle to enhancing CCPs’ revenue, primarily due to the intricate relationship between resource utilization and revenue. Additionally, the substantial scale of CCPs magnifies the difficulties of time-intensive scheduling. To tackle these challenges, we propose Seer, a proactive revenue-aware scheduling system for live streaming services in CCPs. The design of Seer is motivated by meticulous measurements of real-world CCPs environments, which allows us to achieve accurate revenue modeling and overcome three key obstacles that hinder the integration of prediction and optimal scheduling. Utilizing an innovative Pre-schedule-Execute-Re-schedule paradigm and flexible scheduling modes, Seer achieves efficient revenue-optimized scheduling in CCPs. Extensive evaluations demonstrate Seer’s superiority over competitors in terms of revenue, utilization, and anomaly penalty mitigation, boosting CCPs revenue by 147% and expediting scheduling $3.4\times$ faster.

I. INTRODUCTION

The increasing popularity of live streaming services can be attributed to the widespread availability of high-speed networks (e.g., LTE/5G) and advanced personal devices (e.g., iPhone 14 Pro). As a result, live streaming has become one of the most prevalent applications in recent years (e.g., Twitch and TikTok). According to a Zippia report [1], live streaming services accounted for 17% of global IP traffic in 2022 and are projected to grow at a rapid pace. In addition, live streaming has become an essential part of many internet users’ daily routines, with the report [1] showing that people spend 550 billion hours watching live streams in 2021.

This surge in live streaming services has led to the emergence of Crowdsourced Cloud-edge service Platforms (CCPs) that cater to the increasing demands. As illustrated in Fig. 1, the CCP services various live streaming platforms (LSPs) and integrate idle heterogeneous computing and bandwidth resources from resource providers (RPs). Owing to its unique crowdsourcing characteristics, CCPs can expand server coverage for LSPs at a lower cost while enhancing end-users’

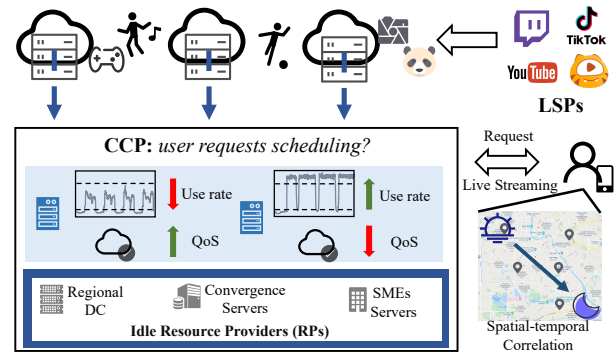


Fig. 1. Crowdsourced Cloud-edge service Platform.

Quality of Experience (QoE) through closer proximity services [2]. The ability to schedule live streaming requests is at the core of CCPs’ Platform-as-a-Service (PAAS) offering for LSPs, acting as a proxy and managing a portion of LSPs’ service capabilities. As such, scheduling plays a decisive role in CCPs’ Quality of Service (QoS) and revenue [3].

In the context of existing geographic proximity-based scheduling strategies being overly simplistic, numerous studies have begun to employ data analysis and prediction of massive scheduling log data to develop optimization strategies or algorithms for achieving more optimal scheduling, such as frameworks aimed at maximizing user QoE or minimizing platform costs [4]–[9]. Although effective, these studies have offered minimal help in improving the revenue of CCPs. As a third-party matchmaking platform, CCPs consolidate a substantial amount of idle resources and strive to maximize their revenue by expanding the scale of services provided on these resources. Therefore, improving resource utilization is the key to increasing CCPs’ revenue.

In fact, the resource utilization promotion brings benefits to all three parties involved: CCPs, LSPs, and RPs. For LSPs, higher utilization means that more requests can be processed at a lower cost [7]. For crowdsourced RPs, higher utilization translates to increased income, thus boosting their engagement. As can be seen, a good resource utilization optimization schedule can promote the thriving development of the entire

*Xiaofei Wang is the corresponding author.

crowdsourced live streaming service ecosystem.

Nonetheless, tackling this issue is highly challenging due to the intermediary nature of CCPs. There exists a complex, non-linear relationship between server resource utilization and CCPs' revenue, which is significantly influenced by RPs' engagement and the QoS Service Level Agreements (SLA) from LSPs. Existing works fall short in addressing this issue and are ill-suited to the revenue optimization task.

Furthermore, as CCPs act as the scheduling proxy for LSPs, the time consumed in generating and executing scheduling strategies is crucial, an aspect often overlooked in prevailing research. Although scheduling models are becoming increasingly sophisticated, the user-perceived latency can significantly increase if the scheduling process takes an extended time. Given that CCPs need to handle numerous heterogeneous servers and diverse live streaming requests simultaneously, the time cost within such a vast scheduling space is formidable.

Anticipating the distribution of incoming requests is a potential method to enhance scheduling efficiency [10]–[12]. However, existing methods struggle to integrate request prediction with actual scheduling. This process mainly encounters three obstacles: 1) The inability to simultaneously predict multiple heterogeneous characteristics of requests. 2) Difficulty in foreseeing the revenue of deploying requests on heterogeneous servers. 3) The challenge of dealing with the discrepancies between predicted and actual request distributions. Additionally, the real-world CCP environment's intense spatiotemporal fluctuations complicate request prediction itself.

To tackle these challenges, we propose a comprehensive solution that focuses on refining the scheduling process to augment CCP revenue. Specifically, we employ a large-scale dataset of real-world live streaming services in CCP to model the intricate relationship between resource utilization and CCP revenue. Furthermore, we introduce Seer, a proactive revenue-aware live streaming scheduling system. Seer successfully integrates request prediction with scheduling optimization, leveraging an innovative **Pre-schedule-Execute-Re-schedule (PER)** paradigm to attain efficient revenue optimization. Simultaneously, it ensures maximal revenue for CCP, and scheduling efficiency, whilst offering flexible configuration options. Our contributions are summarized as follows:

- (i) To the best of our knowledge, we are the first to focus on the revenue optimization of CCPs serving the emerging live streaming industry.
- (ii) Utilizing a comprehensive dataset from real-world CCP operations, we devise a nuanced model that delineates the relationship between resource utilization and CCP revenue. This process also involves an in-depth analysis of requests and allows us to identify and isolate critical features that impact scheduling issues.
- (iii) We introduce Seer, a proactive revenue-aware scheduling system that combines request prediction and scheduling optimization through a novel Pre-schedule-Execute-Re-schedule paradigm. Evaluations based on real-world data demonstrate that Seer significantly enhances CCPs revenue and reduces time costs.

II. RELATED WORK

LSPs and Crowdsourced Cloud-edge Architectures. The rapid expansion of live streaming services can be attributed to the technological advancements in multimedia delivery services [13], [14]. From a technological standpoint, LSPs encompass a video delivery service that records and broadcasts media content to all users in real time. The coexistence of simultaneous content generation and user playback presents substantial challenges for server transmission quality [15].

To address these challenges, LSPs have started employing CCPs to reduce content distribution costs and get lower delivery latency [16], [17]. By integrating widespread idle computing and transmission resources from RPs, CCPs offer a promising solution for LSPs. Compared to providing standardized servers [18], it is more common for CCPs to serve as an independent platform handling requests for LSPs (PaaS) [19]. In a PaaS setup, LSPs directly forward requests to CCPs, which then select the most optimal server. In this regard, CCPs can be viewed as service proxies for LSPs [7].

Analogous to LSPs, CCPs face the challenge of handling massive requests with limited resources. The situation is even more demanding for CCPs, as they must guarantee the LSPs' QoS SLA, while ensuring the engagement of RPs [20], [21].

Optimization Strategies for Live Streaming Service Platforms have garnered considerable attention from both the research community and industry since they provides more significant improvements at lower costs than modifying transfer protocols and architectures [22]. Current industry scheduling mainly rely on geography-based assignment, neglecting request characteristics and factors like QoS and QoE [23].

To address these issues, some studies have proposed improved scheduling strategies. Zhu et al. [20] utilizes decision trees to capture user video engagement, mapping requests to maximize overall QoE. Zhang et al. [24] implements peer-to-peer transmission and proactive high-demand content distribution to decrease server bandwidth usage. Zhang et al. [7] suggests aggregating dispersed audiences and assigning them to fewer pre-selected nodes to reduce bandwidth costs. More studies focus on guaranteeing QoE while lowering service costs. Some suggest adaptive content uploading and edge prefetching strategies [4], [6], while others propose deep reinforcement learning-based (DRL) edge-assisted multicast frameworks for real-time request decisions [25]–[28].

Although effective, these methods fall short when applied to the revenue-optimized scheduling of CCPs due to two factors. 1) The intermediary nature of CCP necessitates a simultaneous consideration of LSPs' QoS SLA and RPs' engagement, leading to a complex nonlinear relationship between resource utilization and revenue. 2) CCPs are confronted with a vast number of servers and diverse requests. Current real-time scheduling strategies (e.g., the DRL-based frameworks) may introduce scheduling latency that is formidable.

III. MEASUREMENTS AND MOTIVATIONS

In this section, we shed light into the following questions:

- Describe the dataset, QoS metrics and request revenue.

- Validate potential improvement and optimal revenue range.
- Examine the spatialtemporal dependencies of requests.
- Investigate the features affecting the request revenue.

By addressing these questions, we aim to gain insights that enable the modeling of the link between resource utilization and CCPs revenue, and facilitate the construction of a robust scheduling framework.

A. Dataset Description and Features Describing

Our research is conducted in collaboration with a leading CCP in China, which consists of 5174 servers distributed across the country and serves more than five typical LSPs. With the CCP’s assistance, we collected three types of data:

- (i) **Live streaming service logs (LL):** We collected 10 days of service logs from all servers dedicated to live streaming. This dataset contains 17854 live streaming channels, 476 unique server IDs (which can be linked to server attributes, such as bandwidth and location), and 500 million requests (with a specific channel and bitrate) across 59 locations. For each unique session, the server records the data size transmitted in one-minute intervals.
- (ii) **Client-reported logs:** These logs correspond in time span to the LL dataset. Every 60 seconds, clients upload the total number of requests issued by users and the related metrics, of which we focus on the startup latency as it is the performance metric that best characterizes the QoE.
- (iii) **Server-side logs:** Similar to the client-reported logs, every 60 seconds, the server records all the successfully served requests, and the failed requests due to server overloads, timeouts, or even disconnections (we calculate the error rates of all types of failed requests).

For the sake of convenience, we refer to the startup latency and requests error rates as the server’s QoS, given that they both form the basis for LSPs’ evaluation of the CCP’s QoS SLA. Furthermore, certain studies consider startup delay and related stall metrics as QoS indicators [7], [20]. Besides, we also refine the notion of *request-server revenue*, denoting the *average data throughput per minute for a request on a given server*, herein termed as **request revenue**.

Ethical Considerations: We have taken a series of measures to ensure the ethical use of data. All user information, including user IDs, IP addresses, and even live streaming room IDs, is anonymized. We do not link the service logs to users; instead, we analyze the service logs at the metadata level (such as the request time and content category).

B. Potential Improvement and Optimal Revenue Range

We first investigate the server resource¹ utilization in a typical day. Fig. 2(a) presents the cumulative distribution function (CDF) of the utilization of all edge servers. As the figure illustrates, a majority of servers experience remarkably low utilization; specifically, more than 60% of servers exhibit real-time utilization of less than 20% throughout the day.

¹Given the nature of live streaming services, all references to ‘resources’ in the following sections specifically denote bandwidth.

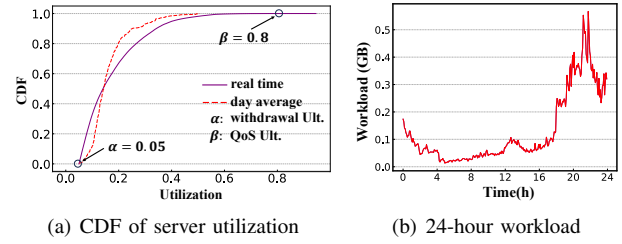


Fig. 2. Server utilization analysis.

Such low utilization is not uncommon for CCPs. Fig. 2(b) shows that the workload volume tend to cluster within two relatively short periods - around noon and evening, while only a handful of requests are observed during the remainder of the day, leading not only to resource wastage but also additional power and operational costs. We argue that such challenges can be alleviated through intelligent recognition of request and scheduling geared towards optimized utilization.

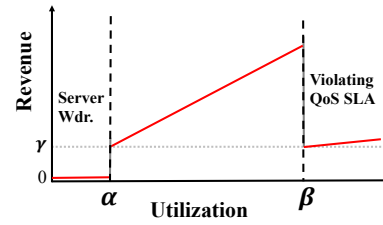


Fig. 3. Fitting plot of server utilization versus revenue.

Besides the potential improvement, we can observe from Fig. 2(a) that server utilization ranges from a lower bound α to an upper bound β (with $\alpha = 0.05$ and $\beta = 0.8$). The presence of the lower threshold can be attributed to the fact that most of CCP’s servers are leased from RPs, who employ the resource utilization as a measure of their revenue. To guarantee a minimum income, RPs set a minimum utilization threshold. If CCP’s scheduling results in server utilization frequently falling below the threshold, RPs may terminate their agreement with CCP and withdraw servers. We refer to this threshold as the server **withdrawal utilization** α .

Due to limitations in network conditions, server hardware and other factors, resource utilization can never reach infinity. As server load increases, the QoS tends to degrade. In practice, CCP signs QoS SLA with LSPs to ensure a minimum QoS. This SLA, reflected in terms of utilization, sets an upper utilization threshold β , which we call the **QoS utilization**.

With the two utilization thresholds, both closely related to CCP’s revenue, we can clearly model the relationship between server resource utilization and CCP’s revenue. From Fig. 3, it is evident that when utilization falls below α , the associated revenue could be negligible due to the risk of server withdrawal². Once server utilization exceeds α , a linearly positive relationship can be established. This implies that CCP’s revenue increases proportionately with the utilization. Finally, upon reaching the QoS utilization β , CCP’s revenue

²Although servers aren’t instantly withdrawn from CCP, the maintenance cost equals or surpasses the server’s gain, resulting in negligible revenue.

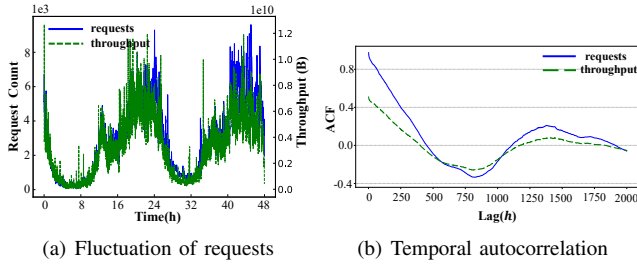


Fig. 4. Temporal fluctuation and autocorrelation analysis.

inevitably diminishes to a lower value γ due to the substantial penalties incurred from violating the QoS SLA. The exact penalty imposed depends on the agreement between CCPs and LSPs. For the sake of modeling, we set γ to fluctuate between 10-30% of the original revenue to represent the penalties LSPs impose on CCPs for SLA violations [29].

In the scheduling process, the CCP aims to stay within a profitable utilization range (optimal revenue range). The withdrawal utilization can be managed by balancing server resources and assigned requests. However, handling the QoS utilization is more complex. This threshold acts as utilization feedback when a QoS SLA is violated, and can't be sufficiently controlled merely by capping tallied utilization. Therefore, it is crucial to establish a mapping from QoS to β to guide the scheduling process (detailed in Section IV-A3).

C. Spatial-Temporal Correlation of Requests

In this part we explore the dependency of requests in both the temporal and spatial domains, thereby offering guidance for subsequent request prediction tasks.

From a temporal perspective (e.g., Fig. 4(a)), requests show periodic variations that align with the day's progression. Moreover, due to the gradual shifts in users' viewing interests and the infrequency of sudden request surges, future requests generally follow a gradual trend based on recent history.

To validate these observations, we employ the *sample AutoCorrelation Function* (ACF) to investigate the temporal dependencies of requests. The ACF quantifies the dependency between values in a sampled process as a function of the time lag h . The ACF calculation procedure for a typical server can be formalized as follows:

$$\rho(h) = \frac{\sum_{t=1}^{D-|h|} (d_{t+|h|} - \bar{d})(d_t - \bar{d})}{\sum_{t=1}^D (d_t - \bar{d})^2}, -D < h < D \quad (1)$$

where d_t is the request volume of time t , and D and \bar{d} are the total count and mean value of sampled requests in the temporal dimension, respectively. The autocorrelation value lies in the range $[-1, 1]$. $\rho(h) = 1$ indicates total positive autocorrelation between data with a time lag of h ; while $\rho(h) = -1$ means total negative autocorrelation.

Fig. 4(b) shows the sample ACF at time lag $h = 0, 1, \dots, 2000$ (unit in minutes) for both requests and throughput. From Fig. 4(b), we can see that the autocorrelation gradually decreases as h increases, i.e., the future request volume depends mainly on the data from the most recent

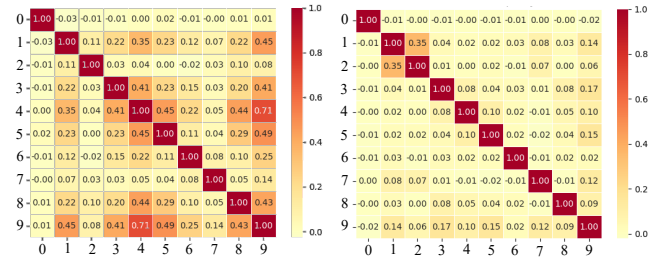


Fig. 5. Spatial correlation analysis.

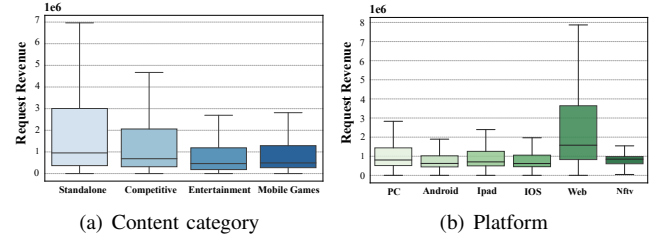


Fig. 6. Influence of different features on request revenue.

historical time. Besides, when the time lag equals 1380 (about one day), the autocorrelation is relatively high. This shows that the requests follows a clear daily pattern. For example, the requests peak and off-peak hours are similar on each day.

On the other hand, we examine the requests correlation in the spatial domain by calculating the Pearson correlation coefficient between two locations:

$$\rho = \frac{\text{cov}(\mathbf{d}_i, \mathbf{d}_j)}{\sigma_{\mathbf{d}_i} \sigma_{\mathbf{d}_j}} \quad (2)$$

where cov is the covariance operator, d_i is the request volumes at location i , and σ is the standard deviation. The magnitude of the Pearson correlation coefficient is the same as ACF.

Fig 5 illustrates the spatial correlation of requests in terms of both the number of requests and data throughput. Specifically, Fig. 5(a) shows a strong positive correlation between the number of requests across different locations, with the correlation coefficient reaching up to 0.71 in some instances.

The preceding analyses confirm the distinct spatialtemporal dependency of requests, prompting us to devise a spatial-temporal prediction model to enhance scheduling efficiency. However, Figures 4(b) and 5(b) indicate that, unlike request volume, data throughput doesn't display similar spatialtemporal patterns as throughput generated by different requests (i.e., request revenue) varies significantly. By investigating features that affects this variation in request revenue, we can obtain a method to foresee request revenue, a crucial factor in combining prediction and scheduling effectively.

D. Principal Factors Affecting Request Revenue

We identify three key features that have the most significant impact on request revenue: a) content category, b) request platform, and c) request timing (peak or off-peak).

Firstly, we classify all requests into four categories based on the live stream channel, as represented in Fig. 6(a), which displays the varying revenue distribution across categories. Notably, requests for competitive gaming content yield higher revenue due to increased bitrate and latency requirements, whereas casual content such as entertainment and mobile game streams generate less revenue.

Another determinant feature is the platform (i.e., the device used for viewing the live stream) since it influences both content type watched and the requested bitrate. As shown in Fig. 6(b), requests emanating from more stable platforms (e.g., PC and Web clients) yield higher revenues compared to mobile platforms (e.g., smartphones and tablets), indicating a preference for higher quality streams on PC and the inherently better network conditions supporting higher data throughput.

Lastly, we consider request timing, specifically whether the request is made during peak hours. As shown in Fig. 7, the revenue per request is typically lower when the number of requests peaks and considerably higher during times with relatively fewer requests. This trend can be attributed to users opting for lower-quality stream bitrates during peak times, and the overall decrease in request revenue due to network fluctuations under high server load.

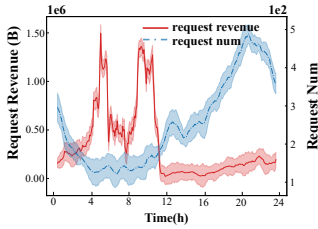


Fig. 7. Influence of request timing.

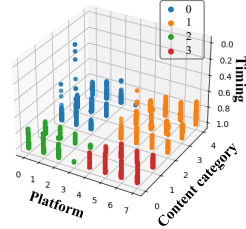


Fig. 8. Distribution of clusters.

Upon observing the profound influence of these features, we are now positioned to foresee request revenue before the requests are actually served (detailed in Section IV-A2). However, implementing this with the predicted requests is challenging due to the difficulty in concurrently perceiving several request features. To address this, we propose to incorporate heterogenous feature information into request categories via clustering. Specifically, we cluster requests into various categories based on content, platform, and timing, thereby allowing us to predict the volume of each category without needing to forecast individual request features, substantially simplifying the prediction task.

We adopt KMeans for clustering, given its suitability for our scenario with distinct separations across features. Fig. 8 illustrates the request point distribution for $k = 4$ clusters. This demonstrates well-defined separation along the three axes, forming distinct and cohesive clusters. However, we stress that $k = 4$ is not our ultimate cluster choice as we must ensure a sufficient number of categories to encapsulate adequate feature information for downstream request revenue prediction.

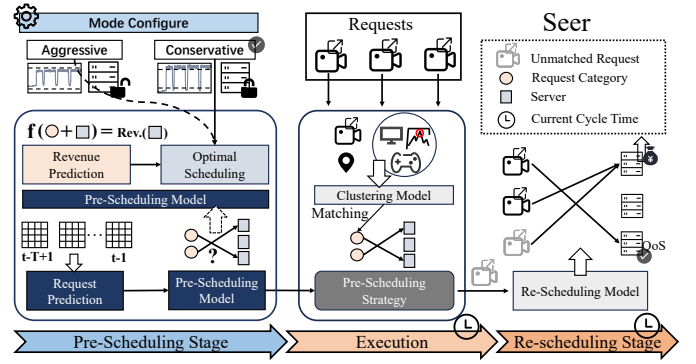


Fig. 9. The system overview of Seer.

IV. SYSTEM OVERVIEW

Fig. 9 provides the overview of Seer. Seer is a proactive revenue-aware live streaming scheduling system, explicitly designed to maximize CCP revenue while addressing related concerns including server withdrawal and QoS SLA. Additionally, Seer emphasizes maximizing efficiency by minimizing the proportion of decision-making time in each scheduling cycle, thereby reducing user-perceived latency caused by scheduling.

Specifically, Seer operates through a three-stage process: pre-scheduling, execution, and re-scheduling. In the pre-scheduling stage, before the actual requests arrive, Seer anticipates the category, volume, and geographic distribution of subsequent requests. This prediction enables a proactive approach to solving a revenue maximization problem under certain constraints, creating an optimal pre-scheduling strategy.

The prediction and problem-solving stages, being the most time-consuming in Seer's execution, are expedited by completing pre-scheduling prior to actual scheduling, effectively reducing user wait times for services.

Upon the actual scheduling cycle, Seer matches and schedules requests according to the pre-scheduling strategy, leaving only a minor proportion of requests (untreated due to prediction errors) for the re-scheduling stage, where they are managed through a simple and efficient scheduling strategy. Beyond these, Seer also employs two optional scheduling configuration modes: conservative and aggressive modes.

A. Proactive Pre-scheduling Stage

As the core stage of Seer, the pre-scheduling stage is composed of the following parts, as shown in the Fig. 10:

1) *Request Prediction Model*: Prior to new scheduling cycle, Seer first predicts the request category distribution of all M locations: $\mathcal{R} = \{R_m | m \in [1, M]\}$ from the prediction model, where $R_m = \{r_m^1, \dots, r_m^N\}$ denotes the number of requests of all N categories in region m .

We introduce a proactive deep learning model that combines an AutoEncoder (AE) with a Gated Recurrent Unit (GRU) for spatial-temporal feature extraction and prediction of live streaming request matrices. The model incorporates the strength of AEs in spatial feature learning with the prowess of GRUs in capturing temporal dependencies, offering a comprehensive method to interpret spatial-temporal data.

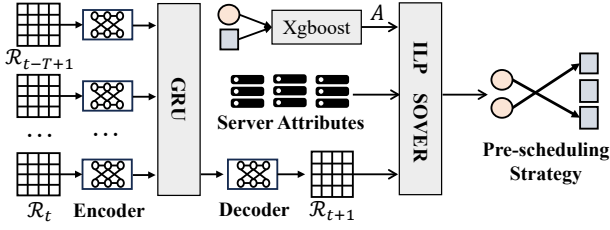


Fig. 10. Process of Seer's pre-scheduling stage.

The architecture of the AE-GRU model (Fig. 10) involves two main components. The first is the AE that learns to transform the spatial relationships across different locations and the request patterns of multiple categories into a compressed representation. The second component is the GRU, which accepts the encoded representation as input and captures the temporal dependencies between sequential matrices. The entire process of the AE-GRU can be defined as follows:

$$\mathcal{H}_t = [\mathbf{En}(\mathcal{R}_1), \dots, \mathbf{En}(\mathcal{R}_t)] \quad (3)$$

$$\mathcal{H}_{t+1} = \mathbf{GRU}(\mathcal{H}_t) \quad (4)$$

$$\hat{\mathcal{R}}_{t+1} = \sigma(W_d \cdot \mathcal{H}_{t+1} + b_d) \quad (5)$$

where \mathcal{R}_t is the input matrix at time t , and $\mathbf{En}(\mathcal{R}_t) = \sigma(W_e \cdot \mathcal{R}_t + b_e)$ is the encoded representation. σ represents the activation function (we use the ReLU function here), W_e and W_d are the weight matrices, and b_e and b_d are bias vectors for the AE-encoder and AE-decoder respectively. Given our use of the standard GRU, for brevity, we adopt **GRU** to represent the standard computational process inherent in the GRU.

By combining these components, AE-GRU is capable of effectively learning both the spatial and temporal features embedded in the request matrices and predicting the future request distribution. Besides, an inherent advantage of the AE-GRU is its capability of efficient feature extraction through a lightweight network structure, which is particularly valuable in real-time scheduling where every second counts.

2) *Modeling Request Revenue*: In this part, we outline our approach to foreseeing request revenue, which accounts for both request features and server attributes. As discussed in Section III-D, intrinsic request features will affect the request revenue. However, server attributes, e.g., bandwidth and geographical location, also affect revenue by influencing transmission stability and speed.

To accurately model request revenue, we employ eXtreme Gradient Boosting (Xgboost), a scalable Gradient Boosted Decision Tree model. Specifically, we use request category, location, server ID, bandwidth, and location as inputs, with the corresponding request revenue as the label. Training Xgboost on ample historical data allows it to model request revenue effectively. To boost scheduling efficiency, we generate the request revenue matrix $\mathbf{A} \in \mathbb{R}^{E \times M \times N}$ in advance by iterating over all request-server combinations on the trained Xgboost:

$$\mathbf{A}_{e,m,i} = \mathbf{Xgboost}(i, m, e, B_e, L_e) \quad (6)$$

$$(e \in [1, E], m \in [1, M], i \in [1, N])$$

where **Xgboost** represents the revenue modeling process, i, m, e, B_e, L_e are corresponding input features, E represents the number of servers, and M and N are defined as before. Xgboost is not only efficient but also generalized, aiding the of request-server combinations unseen in the historical data.

3) *Pre-scheduling Model*: With the predicted request matrix $\hat{\mathcal{R}}_{t+1}$, the core task of Seer in the pre-scheduling stage is to generate a strategy for potential requests in conjunction with the current server states, to ensure in advance that the next cycle of request scheduling is revenue-optimized.

We formally define the revenue-optimized scheduling problem: assuming that there are E edge nodes and M locations. The bandwidth capacity and location of server e is represented as B_e and L_e . We represent the Pre-scheduling Strategy with $PS = \{x_{m,i}^e | e \in [1, E], m \in [1, M], i \in [1, N]\}$, where $x_{m,i}^e$ denotes the number of request of category i from location m served by server e . To this end, the pre-scheduling problem at each scheduling cycle is:

$$\max \sum_{e=1}^E \left(\sum_{m=1}^M \sum_{i=1}^N \frac{x_{m,i}^e * \mathbf{A}_{e,m,i}}{B_e} \right) \quad (7)$$

$$\text{s.t. } x_{m,i}^e \geq 0 \quad (e \in [1, E], m \in [1, M], i \in [1, N]) \quad (8a)$$

$$\sum_{e=1}^E x_{m,i}^e = \hat{r}_m^i \quad (m \in [1, M], i \in [1, N]) \quad (8b)$$

$$\alpha < \sum_{m=1}^M \sum_{i=1}^N \frac{x_{m,i}^e * \mathbf{A}_{e,m,i}}{C_e} < \beta \quad (e \in [1, E]) \quad (8c)$$

where Eq. 7 is our objective function to optimize resource utilization across the CCP, Eq. 8a imposes the constraint on the range of x , while Eq. 8b ensures that all requests are scheduled. Eq. 8c ensures that the utilization of each server remains within the optimal revenue range, thus avoiding server withdrawal or violating QoS SLA.

Given that excessive server workload can lead to significant QoS degradation, we count the historical QoS data in conjunction with servers' bandwidth utilization to ascertain an appropriate value for β . Initially, we calculate CDF for both QoS metrics. To ensure neither metric was excessively poor, we designate β as the smaller utilization that corresponds to the 80th percentile in both QoS metrics:

$$\beta = \min\{U_{Lat_{80}}, U_{Err_{80}}\} \quad (9)$$

where $U_{Lat_{80}}$ and $U_{Err_{80}}$ correspond to the 80th percentile of the startup latency and error rates, respectively.

Since x in Eq. 7 represents non-negative integers, and both the objective function and all constraints are linear, the problem constitutes an Integer Linear Programming (ILP) problem. Although ILP problems can theoretically be solved with an analytical solution, solving ILP is NP-Hard [30]. Considering the enormous scale of CCP's servers and requests, which results in a huge solution space ($E * M * N$ is 800,000+), most ILP solutions can't deliver in time.

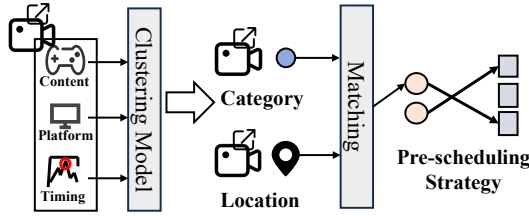


Fig. 11. The process of execution stage.

To circumvent this issue, we propose to reduce dimensionality from the location dimension since it has less effect on request revenue. Specifically, we ignore the request location during the ILP resolution ($x_{m,i}^e \rightarrow \bar{x}_i^e$, representing the number of category i requests assigned to server e from all locations). We also average \mathbf{A} , reducing it to $\bar{\mathbf{A}} \in \mathbb{R}^{E \times N}$, representing the average revenue when server e serves category i requests. Consequently, Eq. 7 simplifies to:

$$\max \sum_{e=1}^E \left(\sum_{i=1}^N \frac{\bar{x}_i^e * \bar{\mathbf{A}}_{e,i}}{B_e} \right) \quad (10)$$

and the constraints of Eq. 8 can be similarly simplified. The complexity of the new ILP is reduced by $M = 59$ times (from one minute to 1s or less). Moreover, we relax the integer constraint on x , turning the problem into a Linear Programming problem. We then use the Branch and Cut (BC) algorithm [31] to solve it. After obtaining the intermediate result \bar{PS} , we perform two processing steps to expand it:

1) Round \bar{PS} to the nearest integer. 2) Expand the location dimension of \bar{PS} based on the geographic distribution of $\hat{\mathcal{R}}_{t+1}$, i.e., divide $\bar{PS} \in \mathbb{R}^{E \times N}$ to $PS \in \mathbb{R}^{E \times M \times N}$ according to the proportion of request in different locations, ensuring:

$$\frac{x_{m,i}^e}{\bar{x}_i^e} = \frac{\sum_{i=1}^N \hat{r}_m^i}{\text{SUM}(\hat{\mathcal{R}}_{t+1})} \quad (11)$$

where $\text{SUM}(\hat{\mathcal{R}}_{t+1})$ represents the number of requests. Despite the risk of reducing expected revenue due to the simplification, we deem this step essential, as Seer needs to ensure the completion of pre-scheduling before actual requests arrive.

B. Pre-strategy Execution Stage

Once the PS is constructed, Seer proceeds to reconcile the real-time incoming requests with the preconceived strategy and schedules them accordingly (as illustrated in Fig. 11).

With the arrival of actual requests, Seer classify them into predefined categories by the clustering model. Then, for each respective location and category, the requests are dispatched to servers in accordance with the pre-scheduling strategy.

The request matching can be formalized as $f(\mathcal{R}_{t+1}, PS) \rightarrow S$, where f is the matching function, \mathcal{R}_{t+1} is the actual request matrix, and $S = \{s_{m,i}^e | e \in [1, E], m \in [1, M], i \in [1, N]\}$ is the adapted scheduling strategy. Specifically, f allocates requests of category i from location m to server e , according to the magnitude and order of $x_{m,i}^e$ in PS , ensuring that servers with greater serving capacity $x_{m,i}^e$ are satisfied first.

Additionally, as actual requests deviate from the prediction, leading to a discrepancy between the number of requests and the number allocated in PS . To counter this, Seer adopts a *request priority* principle, whereby if requests exceed the allocated quantity, the surplus is logged for subsequent handling. Conversely, if requests are fewer, servers that were not assigned the requisite number of requests are ignored, ensuring that $\sum_{e=1}^E s_{m,i}^e \leq r_m^i$. The unmatched requests will be further handled in the re-scheduling stage.

C. Re-scheduling Stage

In this stage, Seer assigns the remaining unserved requests according to CCP's original heuristic scheduling method, which schedules requests to the servers that is closest and has the most remaining bandwidth. The remaining bandwidth, B_e^{remain} , is computed using the updated scheduling strategy S , and revenue matrix A , such that $B_e^{\text{remain}} = B_e - \sum_{m=1}^M \sum_{i=1}^N s_{m,i}^e * A_{e,m,i}$. Upon completing this heuristic scheduling, Seer successfully schedule all actual requests.

Essentially, Seer operates cyclically, beginning with pre-scheduling, progressing to execution and re-scheduling, and then starts the next cycle based on the revised server state and requests. Given that Seer's execution and re-scheduling stages involve minimal computations, it allocates considerable time for the next-cycle's pre-scheduling.

Notably, throughout long-term operation, Seer will update its components and parameters, including the clustering model, the request and revenue prediction models, and the QoS utilization β .

D. Flexible Scheduling Model

We introduce two modes for Seer: Conservative and Aggressive modes. The previous settings describe Seer's default conservative mode, which prioritizes RPs' engagement and prevents server withdrawal. However, under certain circumstances, the more lucrative Aggressive mode is preferable for higher CCP revenue and lower server operational costs, despite potential server withdrawal. This mode modifies Seer's pre-scheduling and re-scheduling stages. During pre-scheduling, Seer discards the minimum utilization constraint in Eq. 8c and ignores servers with utilization $< \alpha$ in Eq. 7. During the re-scheduling, Seer checks the potential server utilization, discards all servers with utilization $< \alpha$, and reallocates their requests to the remaining servers with the lowest utilization.

V. PERFORMANCE EVALUATION

A. Experiment Setup

1) *Implementation Details*: The evaluation of Seer is based on simulated scheduling of real requests from the three real datasets discussed in Section III. The whole process ensures that the scheduling mechanism is anchored on actual CCPs scheduling situation. Specifically, our experiments involve processing over 500 million live-streaming requests spanning 10 days, from February 5th to 14th, 2023, and the data is selected

¹As the time comes to day2 (weekend), the scale of requests increases significantly.

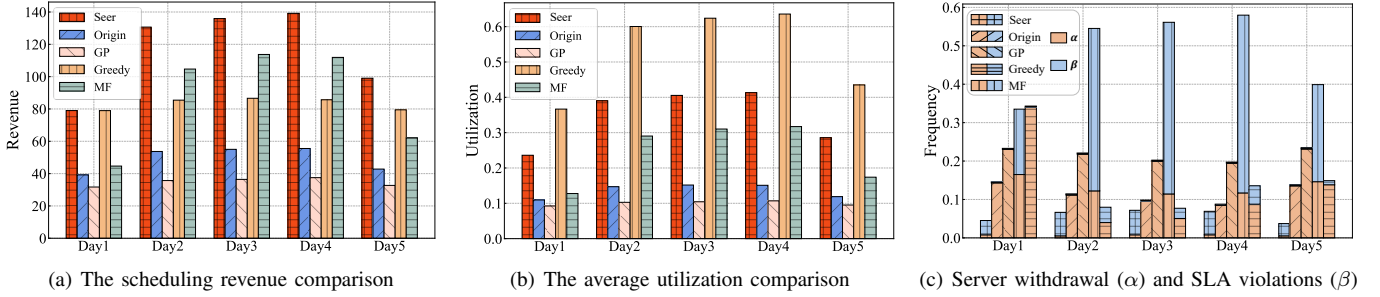


Fig. 12. Scheduling performance comparison¹.

for covering a complete natural week to demonstrate the model’s performance under different magnitude fluctuations.

The data from the first five days are utilized to carry out the CCP measurements and verify the setup of Seer, and the last five days are used to test the scheduling performance. Based on the analysis in Section III-A, we set the request cluster number $k = 29$, $\alpha = 0.05$, and β fluctuates in 0.7 to 0.9 with the operation of the CCP. Besides, we calculate the server revenue with a utilization of U by the following function:

$$\text{rev}(U) = \begin{cases} 0, & U < \alpha, \\ 0.2U, & U > \beta, \\ U, & \text{otherwise.} \end{cases} \quad (12)$$

The setting of 0 and $0.2U$ is follow the analysis of anomaly penalties in Section III-B. To simplify the model, we disregard the potential price variances across different RPs and LSPs. The decision interval of Seer is set as 1 min, which is intended to be consistent with real-world CCP settings.

2) Baselines:

- Heuristic method (Origin): This method schedules requests to the nearest servers with maximum remaining bandwidth. Its the origin scheduling method of our collaborated CCP, and we do not perform additional replication but only record the relevant metrics under the real CCP.
- Geographically-Proximate (GP): This approach schedules requests to the nearest available edge servers. It is the most prevalent method in industry.
- Revenue-aware Greedy (Greedy) [6]: This method is based on the request revenue matrix \mathbf{A} . It allocates requests to the server that yields the highest revenue until the server’s bandwidth capacity is reached. It can be regarded as the upper-bound in the context of utilization.
- Maximum-flow (MF) [32], [33]: This kind of algorithms convert the scheduling problem into a flow control problem (the server is treated as the graph node, the constrained bandwidth is treated as the link capacity, and the scheduled request revenue is treated as the flow).

All models undergo evaluation on a unified scheduling decision server, handling requests of the same scale. This setup guarantees a fair and equitable comparison between different models while ensuring that the time consumption of each algorithm is consistently measured and comparable.

B. Scheduling Performance

1) *CCP Revenue*: We conduct continuous scheduling over the last five days and compare the performances of the Seer and other baselines. As can be seen in Fig. 12(a), Seer consistently outperforms all baselines across the five testing days, showcasing superior revenue due to its optimized scheduling policy that expertly manages server resources within the optimal range for maximizing revenue.

Specifically, compared to the original heuristic method, Seer manifests an enhancement of 147% in the average revenue. Against the GP method, the improvement of Seer is even more substantial, almost $4\times$ the GP revenue. Though falling marginally short of Seer (30% revenue reduction), the MF method still outperforms the other approaches.

Regarding average resource utilization (Fig. 12(b)), the Seer achieves the highest reasonable utilization (second only to Greedy’s upper-bound). The Greedy method exhibits a higher utilization owing to its inherent scheduling mechanism that favors servers with the highest potential revenue. However, the non-linear relationship between revenue and utilization often leads to the Greedy method surpassing the QoS utilization β , thereby diminishing its revenue.

Examining schedule principles, the Greedy and GP methods focus on short-term or local optimization, overlooking overall resource allocation and revenue-related constraints. In contrast, the Seer and MF methods consider the broader network state, yielding more balanced utilization and higher revenue.

2) *Server Withdrawal and QoS SLA*: Fig. 12(c) shows the server withdrawal and QoS SLA violations frequency of different methods’ scheduling. In terms of the combination of those both metrics, Seer demonstrates clear advantages by consistently optimizing scheduling to maintain server utilization within the optimal revenue range (i.e., $\alpha < U < \beta$).

Analyzing the frequency of server withdrawal (α in Fig. 12(c)), the Origin and GP methods demonstrate higher withdrawal, up to 23% for GP and 14% for Origin, due to their conservative nature which results in extremely low utilization.

The Greedy method shows a reversal trend, demonstrating the highest QoS SLA violations (up to 46%) since it locally optimizes the utilization. Meanwhile, the MF’s performance fluctuates with varying request scales. Notably, at smaller scales, MF is prone to server withdrawal, and inversely, it’s susceptible to QoS SLA violations at larger scales.

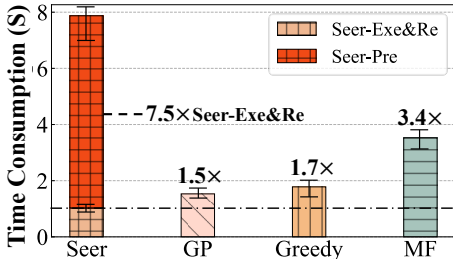


Fig. 13. Average scheduling time consumption.

Despite the superiority of Seer, it is not entirely immune to server withdrawal and QoS SLA violations due to the existence of prediction errors and the approximation in the pre-scheduling stage. However, these occurrences are minimal and reflect the balance achieved by the Seer between maximizing CCP revenue and ensuring system efficiency.

3) *Scheduling Efficiency*: We compare the average time consumption for each scheduling cycle of different methods. As illustrated in Fig. 13, Seer exhibits impressive efficiency in scheduling, attributable to its unique prediction and **PER** paradigm. Seer strategically shifts the time-consuming optimization problem-solving step to before the arrival of real-time requests, leaving the time-efficient execution and re-scheduling stages for the actual scheduling cycle. Seer reduces the time consumption for scheduling by 1.5 \times , 1.7 \times , and 3.4 \times compared to GP, Greedy, and MF, respectively.

It's notable that existing state-of-the-art scheduling methods (e.g., [27], [34]), don't fully leverage the predictive advantage. They solve the optimization problem based on real-time requests (similar to Seer's pre-scheduling stage). This choice notably increases user-perceived latency. For example, if Seer conducted pre-scheduling during actual request arrivals, the total scheduling time would inflate by 7.5 \times , despite we have already simplified the optimization process.

C. Discussion of Generalizability

1) *Differences in Scheduling Modes*: To compare the two scheduling modes of Seer, we implement both Seer-C (Conservative mode) and Seer-A (Aggressive mode) on the five-day dataset. As illustrated in Fig. 14(a), Seer-A outperforms Seer-C in generating higher revenue and better resource utilization, and due to the reduction of constraints in the optimization problem, it consumes less time in the pre-scheduling stage but more during the actual scheduling cycle. Fig. 14(b) shows how, in contrast to the origin scheduling strategy, Seer reshapes the resource utilization across CCP servers, optimizing resource use more effectively, which is more evident in Seer-A.

Thus, if CCP owner can tolerate sacrificing some loss in RPs engagement (with Seer-A discarding, on average, 33% of servers) in exchange for enhanced gains, Seer-A often presents a more appealing revenue proposition. However, it does demand trade-off long-term operational balance within the LSPs, CCP, and RPs ecosystem, ensuring an adequate supply of cooperative RPs.

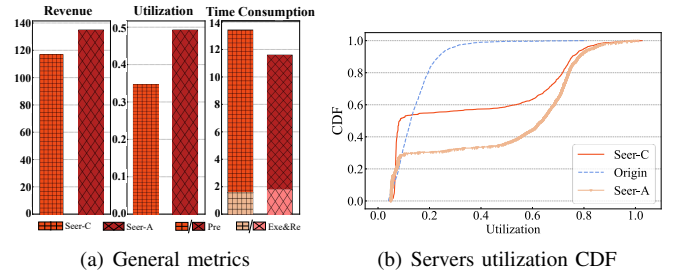


Fig. 14. Comparison of different scheduling modes.

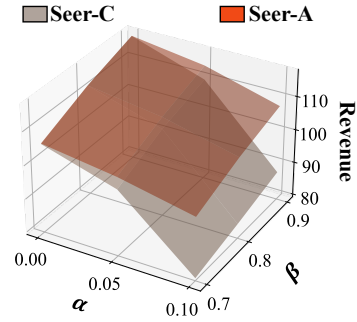


Fig. 15. Variation of revenue with utilization threshold.

2) *Effect of Real-world Parameters*: Fig. 15 depicts the influence of varying α and β thresholds on Seer's revenue. As α increases, signifying RPs' heightened utilization demand, Seer's scheduling scope shrinks, subsequently diminishing CCP's revenue. Conversely, a rise in β gradually improves Seer's revenue as it indicates enhanced network condition and hardware configurations, enabling the servicing of more requests while maintaining QoS. It's worth noting that when $\alpha = 0$, both modes of Seer yield identical revenue. Beyond this instance, Seer-A consistently outperforms Seer-C, given no servers are discarded when $\alpha = 0$, causing Seer-A to revert to a strategy identical to Seer-C.

The findings above suggest that CCPs could be proactive in negotiating with RPs or offering incentives to enhance their engagement (lowering α), and optimize the overall network environment and hardware configurations to increase β . Consequently, CCPs would have a broader scheduling scope to generate greater revenue with limited resources. We argue that such a discussion about this trade-off is of immense value as it contributes to the prosperity of the live streaming ecosystems.

VI. CONCLUSION

This paper introduces Seer, a proactive revenue-aware scheduling system for live streaming services in CCPs. Inspired by our meticulous measurements of real-world CCP environments, by integrating a novel PER paradigm and flexible scheduling modes, Seer exhibits efficient revenue-optimized scheduling in large-scale CCPs. Over five days of testing, Seer demonstrated superior performance, boosting CCP origin revenue by 147% and accelerating scheduling 3.4 \times faster than its counterparts.

ACKNOWLEDGMENT

Thanks to PPIO Cloud Computing (Shanghai) Co., Ltd. for providing the system platform and original logs. This work was supported in part by China NSFC through grant No. 62072332 and China NSFC (Youth) through grant No. 62002260; in part by the Tianjin Xinchuang Haihe Lab under Grant No.22HHXCJC00002.

REFERENCES

- [1] ZIPPAA, "Live streaming statistics 2023: Facts about live streaming in the u.s." 2023. [Online]. Available: <https://www.zippia.com/advice/live-streaming-statistics/>
- [2] M. Xu, Z. Fu, X. Ma, L. Zhang, Y. Li, F. Qian, S. Wang, K. Li, J. Yang, and X. Liu, "From cloud to edge: a first look at public edge platforms," in *Proceedings of the 21st ACM Internet Measurement Conference*, 2021, pp. 37–53.
- [3] F. Wang, J. Liu, C. Zhang, L. Sun, and K. Hwang, "Intelligent edge learning for personalized crowdsourced livecast: Challenges, opportunities, and solutions," *IEEE Network*, vol. 35, no. 1, pp. 170–176, 2021.
- [4] J. Li, Z. Li, Q. Wu, and G. Tyson, "On Uploading Behavior and Optimizations of a Mobile Live Streaming Service," *Proceedings - IEEE INFOCOM*, pp. 1299–1308, 2022.
- [5] C. Zhang, J. Liu, Z. Wang, and L. Sun, "Look Ahead at the First-mile in Livecast with Crowdsourced Highlight Prediction," *Proceedings - IEEE INFOCOM*, pp. 1143–1152, 2020.
- [6] F. Haouari, E. Baccour, A. Erbad, A. Mohamed, and M. Guizani, "QoE-Aware Resource Allocation for Crowdsourced Live Streaming: A Machine Learning Approach," *IEEE International Conference on Communications*, vol. 2019-May, 2019.
- [7] R.-X. Zhang, C. Yang, X. Wang, T. Huang, C. Wu, J. Liu, and L. Sun, "Aggcast: Practical cost-effective scheduling for large-scale cloud-edge crowdsourced live streaming," in *Proceedings of the 30th ACM International Conference on Multimedia*, 2022, pp. 3026–3034.
- [8] J. Jiang, V. Sekar, H. Milner, D. Shepherd, I. Stoica, and H. Zhang, "Cfa: A practical prediction system for video qoe optimization," in *13th USENIX Symposium on Networked Systems Design and Implementation (NSDI 16)*, 2016, pp. 137–150.
- [9] F. Tashtarian, A. Bentaleb, H. Amirpour, B. Taraghi, C. Timmerer, H. Hellwagner, and R. Zimmermann, "Lalisa: Adaptive bitrate ladder optimization in http-based adaptive live streaming," in *NOMS 2023-2023 IEEE/IFIP Network Operations and Management Symposium*, 2023, pp. 1–9.
- [10] T. L. Duc, R. G. Leiva, P. Casari, and P.-O. Östberg, "Machine learning methods for reliable resource provisioning in edge-cloud computing: A survey," *ACM Computing Surveys (CSUR)*, 2019.
- [11] S. Huang, Z. Wang, H. Zhang, X. Wang, C. Zhang, and W. Wang, "One for all: Unified workload prediction for dynamic multi-tenant edge cloud platforms," in *Proceedings of the 29th ACM SIGKDD Conference on Knowledge Discovery and Data Mining*, ser. KDD '23. New York, NY, USA: Association for Computing Machinery, 2023. [Online]. Available: <https://doi.org/10.1145/3580305.3599453>
- [12] S. Huang, H. Zhang, X. Wang, M. Chen, J. Li, and V. C. M. Leung, "Spatio-temporal-social multi-feature-based fine-grained hot spots prediction for content delivery services in 5g era," in *Proceedings of the 30th ACM International Conference on Information & Knowledge Management*, ser. CIKM '21. New York, NY, USA: Association for Computing Machinery, 2021.
- [13] R. Giuliano, F. Mazzenga, and A. Vizzarri, "Integration of broadcaster and telco access networks for real time/live events," *IEEE Transactions on Broadcasting*, vol. 66, no. 3, pp. 667–675, 2020.
- [14] B. Jedari, G. Premsankar, G. Illahi, M. Di Francesco, A. Mehrabi, and A. Ylä-Jääski, "Video caching, analytics, and delivery at the wireless edge: a survey and future directions," *IEEE Communications Surveys & Tutorials*, vol. 23, no. 1, pp. 431–471, 2020.
- [15] N.-N. Dao, A.-T. Tran, N. H. Tu, T. T. Thanh, V. N. Q. Bao, and S. Cho, "A contemporary survey on live video streaming from a computation-driven perspective," *ACM Comput. Surv.*, 2022.
- [16] V. K. Adhikari, Y. Guo, F. Hao, M. Varvello, V. Hilt, M. Steiner, and Z.-L. Zhang, "Unreeling netflix: Understanding and improving multi-cdn movie delivery," in *2012 Proceedings IEEE INFOCOM*. IEEE, 2012, pp. 1620–1628.
- [17] R.-X. Zhang, T. Huang, M. Ma, H. Pang, X. Yao, C. Wu, and L. Sun, "Enhancing the crowdsourced live streaming: A deep reinforcement learning approach," in *Proceedings of the 29th ACM Workshop on Network and Operating Systems Support for Digital Audio and Video*, 2019, pp. 55–60.
- [18] S. S. Manvi and G. Krishna Shyam, "Resource management for infrastructure as a service (iaas) in cloud computing: A survey," *Journal of Network and Computer Applications*, 2014.
- [19] C. Pahl, "Containerization and the paas cloud," *IEEE Cloud Computing*, vol. 2, no. 3, pp. 24–31, 2015.
- [20] G. Zhu and W. Gu, "User mapping strategy in multi-cdn streaming: A data-driven approach," *IEEE Internet of Things Journal*, pp. 6638–6649, 2021.
- [21] C. Anglano, M. Canonico, and M. Guazzone, "Profit-aware resource management for edge computing systems," in *Proceedings of the 1st International Workshop on Edge Systems, Analytics and Networking*, 2018, pp. 25–30.
- [22] A. A. Barakabitze, N. Barman, A. Ahmad, S. Zadtootaghaj, L. Sun, M. G. Martini, and L. Atzori, "Qoe management of multimedia streaming services in future networks: a tutorial and survey," *IEEE Communications Surveys & Tutorials*, vol. 22, no. 1, pp. 526–565, 2019.
- [23] J. Dilley, B. Maggs, J. Parikh, H. Prokop, R. Sitaraman, and B. Weihl, "Globally distributed content delivery," *IEEE Internet Computing*, vol. 6, no. 5, pp. 50–58, 2002.
- [24] Y. Zhang, C. Gao, Y. Guo, K. Bian, X. Jin, Z. Yang, L. Song, J. Cheng, H. Tuo, and X. Li, "Proactive video push for optimizing bandwidth consumption in hybrid cdn-p2p vod systems," in *IEEE INFOCOM 2018 - IEEE Conference on Computer Communications*, 2018, pp. 2555–2563.
- [25] F. Wang, C. Zhang, F. Wang, J. Liu, Y. Zhu, H. Pang, and L. Sun, "Intelligent edge-assisted crowdcast with deep reinforcement learning for personalized qoe," in *IEEE INFOCOM 2019 - IEEE Conference on Computer Communications*, 2019, pp. 910–918.
- [26] R.-X. Zhang, M. Ma, T. Huang, H. Li, J. Liu, and L. Sun, "Leveraging qoe heterogeneity for large-scale livecast scheduling," in *Proceedings of the 28th ACM International Conference on Multimedia*, 2020, pp. 3678–3686.
- [27] F. Wang, C. Zhang, F. Wang, J. Liu, Y. Zhu, H. Pang, and L. Sun, "Deepcast: Towards personalized qoe for edge-assisted crowdcast with deep reinforcement learning," *IEEE/ACM Transactions on Networking*, vol. 28, no. 3, pp. 1255–1268, 2020.
- [28] H. Wang, K. Wu, J. Wang, and G. Tang, "Rldish: Edge-assisted qoe optimization of http live streaming with reinforcement learning," in *IEEE INFOCOM 2020 - IEEE Conference on Computer Communications*, 2020, pp. 706–715.
- [29] F. Faniyi and R. Bahsoon, "A systematic review of service level management in the cloud," *ACM Comput. Surv.*, vol. 48, no. 3, 2015.
- [30] A. Paulus, M. Rolinek, V. Musil, B. Amos, and G. Martius, "Comboptnet: Fit the right np-hard problem by learning integer programming constraints," in *Proceedings of the 38th International Conference on Machine Learning*, ser. Proceedings of Machine Learning Research. PMLR, 2021, pp. 8443–8453.
- [31] J.-F. Cordeau, "A branch-and-cut algorithm for the dial-a-ride problem," *Operations Research*, vol. 54, no. 3, pp. 573–586, 2006.
- [32] X. Chen, C. Xu, M. Wang, Z. Wu, S. Yang, L. Zhong, and G.-M. Muntean, "A universal transcoding and transmission method for livecast with networked multi-agent reinforcement learning," in *IEEE INFOCOM 2021 - IEEE Conference on Computer Communications*, 2021, pp. 1–10.
- [33] A. Sinha and E. Modiano, "Optimal control for generalized network-flow problems," *IEEE/ACM Transactions on Networking*, vol. 26, no. 1, pp. 506–519, 2018.
- [34] R.-X. Zhang, M. Ma, T. Huang, H. Pang, X. Yao, C. Wu, J. Liu, and L. Sun, "Livesmart: A qos-guaranteed cost-minimum framework of viewer scheduling for crowdsourced live streaming," in *Proceedings of the 27th ACM International Conference on Multimedia*, 2019, pp. 420–428.